SUPPLEMENTAL INFORMATION

Title: A functional binding domain in the Rbpr2 receptor is required for vitamin A transport, ocular retinoid homeostasis, and photoreceptor cell survival in zebrafish

Authors: Ashish K. Solanki[1], Altaf A. Kondkar[2], Joseph Fogerty[3], Yanhui Su[1], Seok-hyung Kim[1], Joshua H. Lipschutz[1,4], Deepak Nihalani[1], Brian D. Perkins[3] and Glenn P. Lobo[1,5*].

Affiliations:

[1]Department of Medicine, Medical University of South Carolina, Charleston, SC, 29425, USA. lobo@musc.edu (G.P.L.); solankia@musc.edu (A.K.S.); su@musc.edu (Y.S.); nihalani@musc.edu (D.N.); lipschut@musc.edu (J.H.L.); kims@musc.edu (S.H.K.).

[2]Glaucoma Research Chair, Department of Ophthalmology, College of Medicine, King Saud University, Riyadh, Saudi Arabia. akondkar@ksu.edu.sa (A.A.K.)

[3]Department of Ophthalmic Research, Cole Eye Institute, Cleveland Clinic, Cleveland, OH 44195, USA. fogertj@ccf.org (J.F.); perkinB2@ccf.org (B.P.).

[4]Ralph H. Johnson VA Medical Center, Division of Research, Charleston, SC 29420, USA. lipschut@musc.edu (J.H.L.).

[5]Department of Ophthalmology, Medical University of South Carolina, Charleston, SC, 29425, USA. lobo@musc.edu (G.P.L.)

***Corresponding Author**

Glenn P. Lobo, Ph.D.
Assistant Professor of Medicine
Department of Medicine
70 President Road
Drug Discovery Building DDB513
Charleston, SC 29425
Office: 843-876-2371
Email: lobo@musc.edu

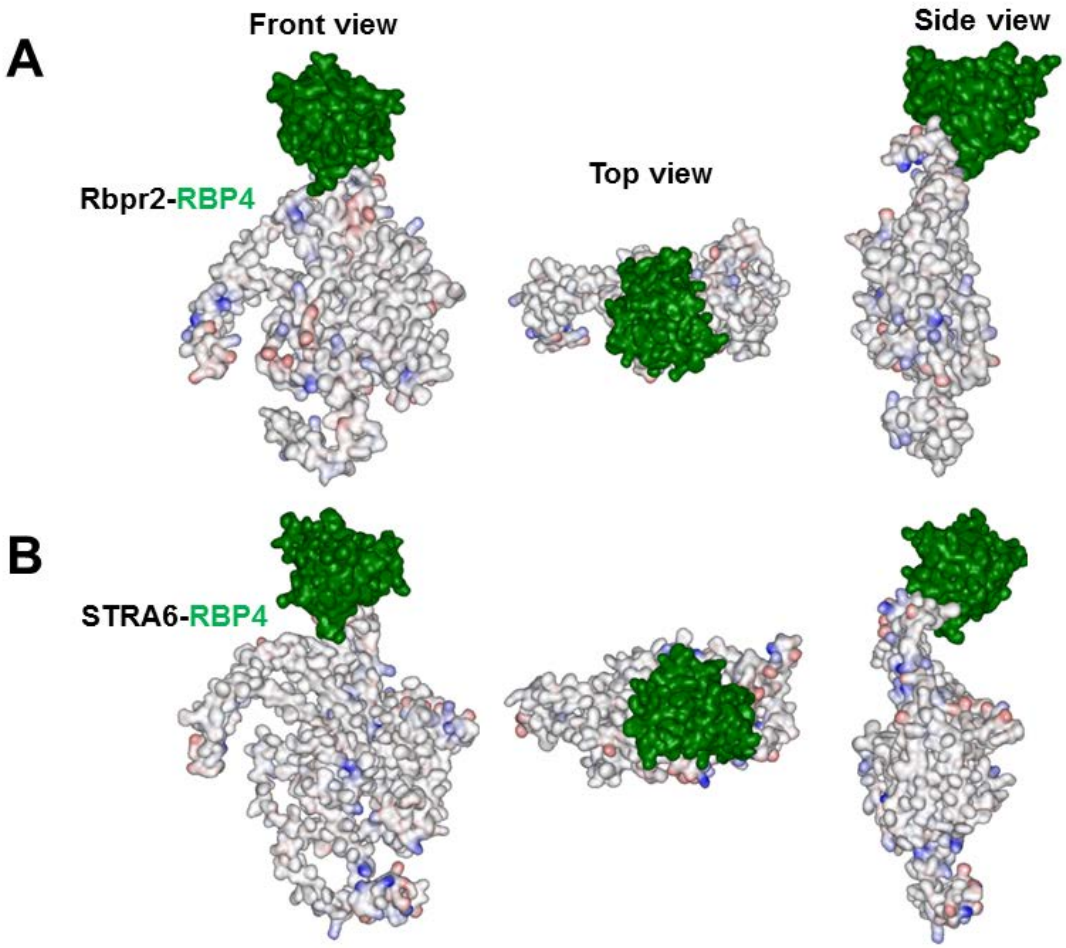

Figure S1. Surface filled view of Rbpr2 and RBP4 protein-protein interactions based on HADDOCK docking analysis.

Multiple surface filled views of (**A**) Zebrafish Rbpr2 with human RBP4, and (**B**) Zebrafish Stra6 with Human RBP4, protein-protein interactions are shown.

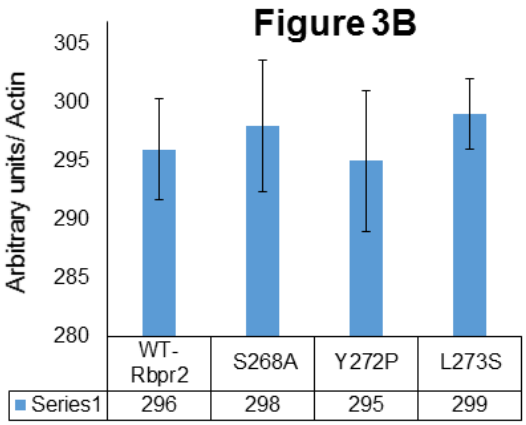

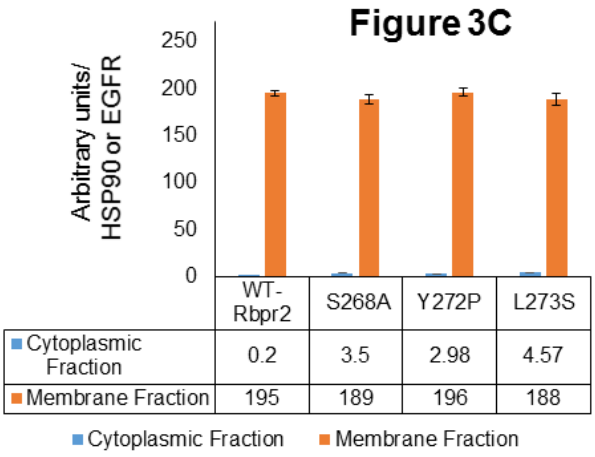

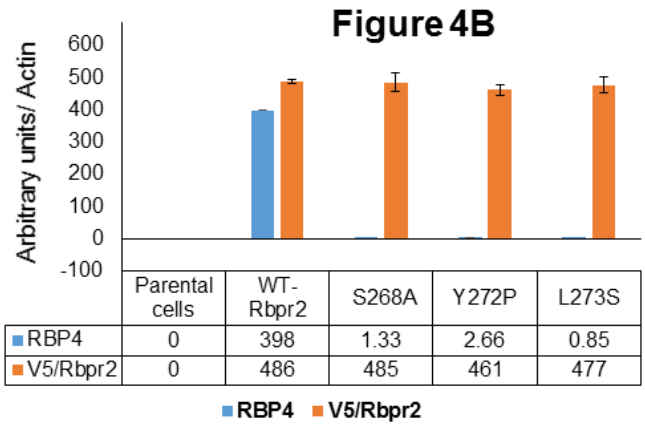

Figure S2. Densitometry analysis of western blots.

Image J software was used to quantify (Arbitrary Units) protein bands from Figures 3B, 3C, and 4B. Analysis is representative from three western blot experiments.

Figure S3. Generation of *rbpr2*-RBP4 binding domain zebrafish mutants.

(**A**) The proposed RBP4 binding domain in zebrafish Rbpr2 was targeted using CRISPR gRNAs (underlined), PAM site shown in green. (**B**) The CRISPR/Cas9 cutting generated multiple mutant alleles. A 1-bp deletion in the zebrafish Rbpr2 (*rbpr2*$^{fs\text{-}muz99}$) coding sequence that results in a frameshift that affects the downstream SYL-RBP4 binding domain was chosen for all further analysis. (**C**) Sequencing chromatograms from wild-type (WT) and *rbpr2*$^{fs\text{-}muz99}$ mutant.

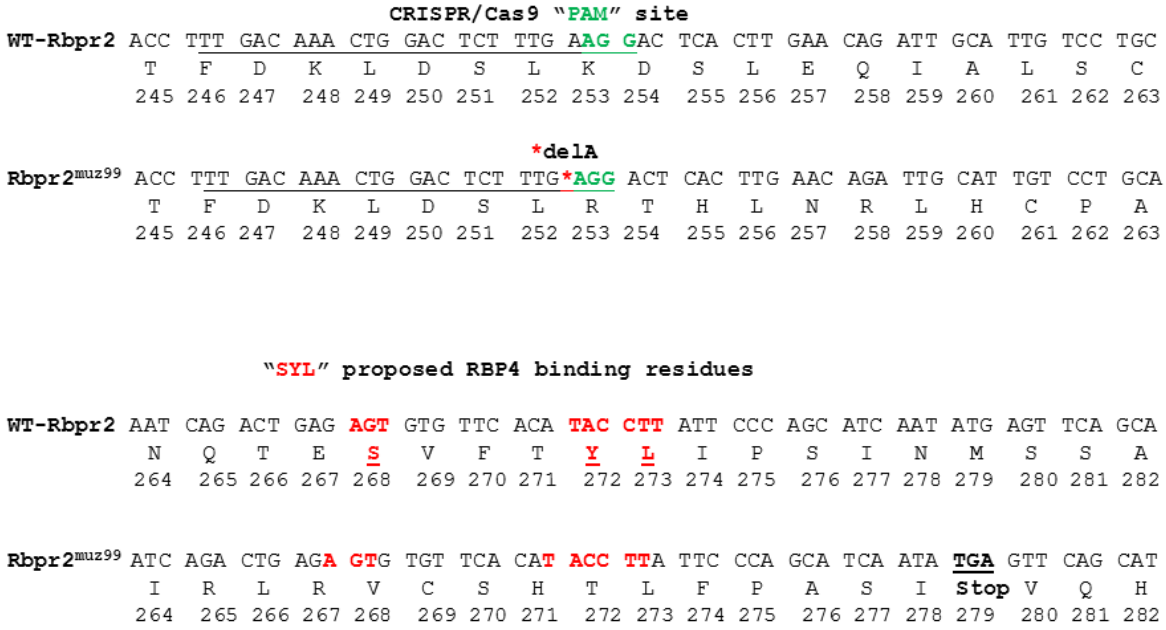

Figure S4. Functional consequences of the CRISPR/Cas9 generated *rbpr2*$^{fs\text{-}muz99}$ mutant zebrafish line.

The 1bp deletion in this *rbpr2* mutant line resulted in a frameshift, and in the downstream disruption of the RBP4 binding residues, resulting in a pre-mature stop codon after the proposed RBP4 functional domain in Rbpr2.

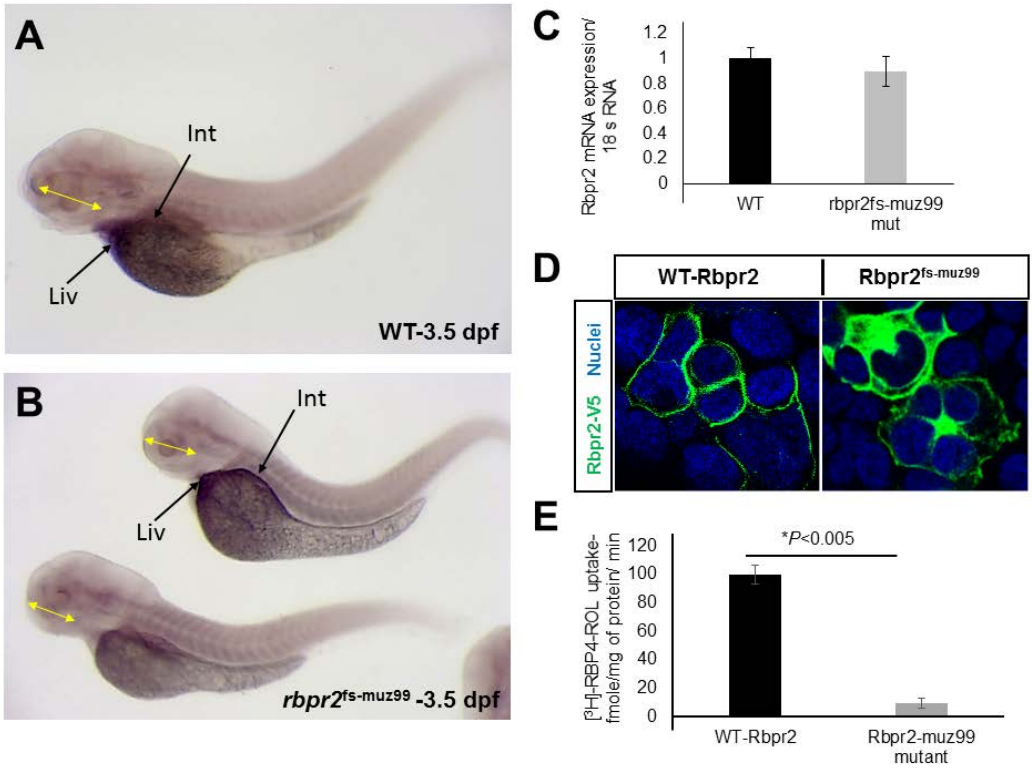

Figure S5. Functional characterization of the *rbpr2*$^{fs\text{-}muz99}$ mutant.

(**A, B**) Rbpr2 mRNA expression patterns in WT-larvae (**A**), and *rbpr2*$^{fs\text{-}muz99}$ mutants (**B**) at 3.5-days post fertilization (dpf) analyzed by whole mount *In-situ* Hybridization (WISH). (**C**) Zebrafish Rbpr2 mRNA expression quantification by Q-RTPCR. (**D**) Functional characterization of the *rbpr2*$^{fs\text{-}muz99}$ mutant by protein localization analysis in NIH3T3 cells. Scale bar=50μm. (**E**) [^{3}H]ROL-RBP4 uptake assays in NIH3T3 cells expressing either WT-Rbpr2 or *rbpr2*$^{fs\text{-}muz99}$ mutant.

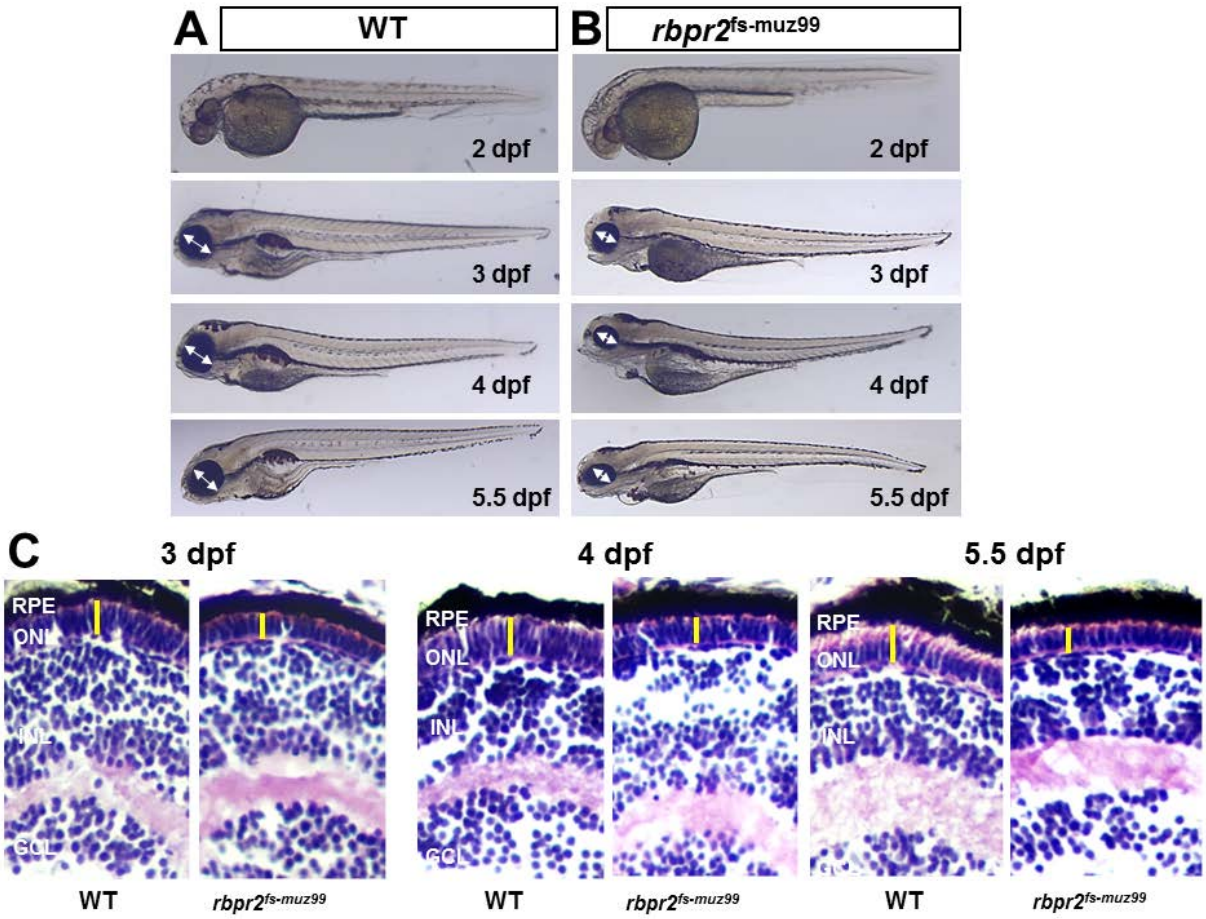

Figure S6. Manifestation of early eye phenotypes in *rbpr2*-RBP4$^{fs\text{-}muz99}$ mutants. Compared to WT animals (**A**), loss of Rbpr2 in *rbpr2*-RBP4 mutant animals (**B**) manifests in early eye phenotypes during developmental stages. Systemic phenotypes in *rbpr2*-RBP4 mutant animals is attributable to general defects in retinoid metabolism during late larval stages. (**C**) Retinal histology and H&E staining of retinas from 3, 4 and 5.5 dpf WT and *rbpr2*-mutants. Photoreceptor outer segments (OS) appear shorter as compared to WT retinas at similar development time-points. Retinal lamination layers in mutants, like in WT larvae, were well preserved at the indicated time points of analysis. OS, outer segments; IS, inner segments; ONL, outer nuclear layer; INL, inner nuclear layer; WT, wild-type; dpf, days post fertilization.

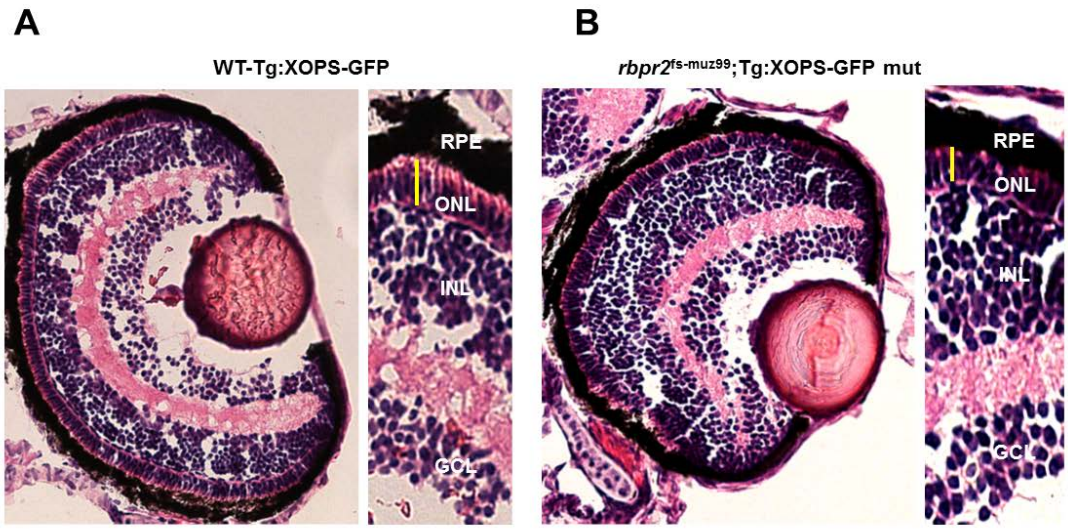

Figure S7. Retinal phenotypes of *rbpr2*$^{fs\text{-}muz99}$;Tg:XOPS-GFP mutant animals at 5.5 dpf.

Compared to WT-Tg:XOPS-GFP zebrafish (**A**), eyes of F3 generation *rbpr2*$^{fs\text{-}muz99}$;Tg:XOPS-GFP mutant animals (**B**) were smaller, and showed shorter photoreceptor layer outer segments by H&E analysis. ONL, outer nuclear layer; INL, inner nuclear layer; GCL, ganglion cell layer; dpf, days post fertilization; RPE, retina pigmented epithelium.

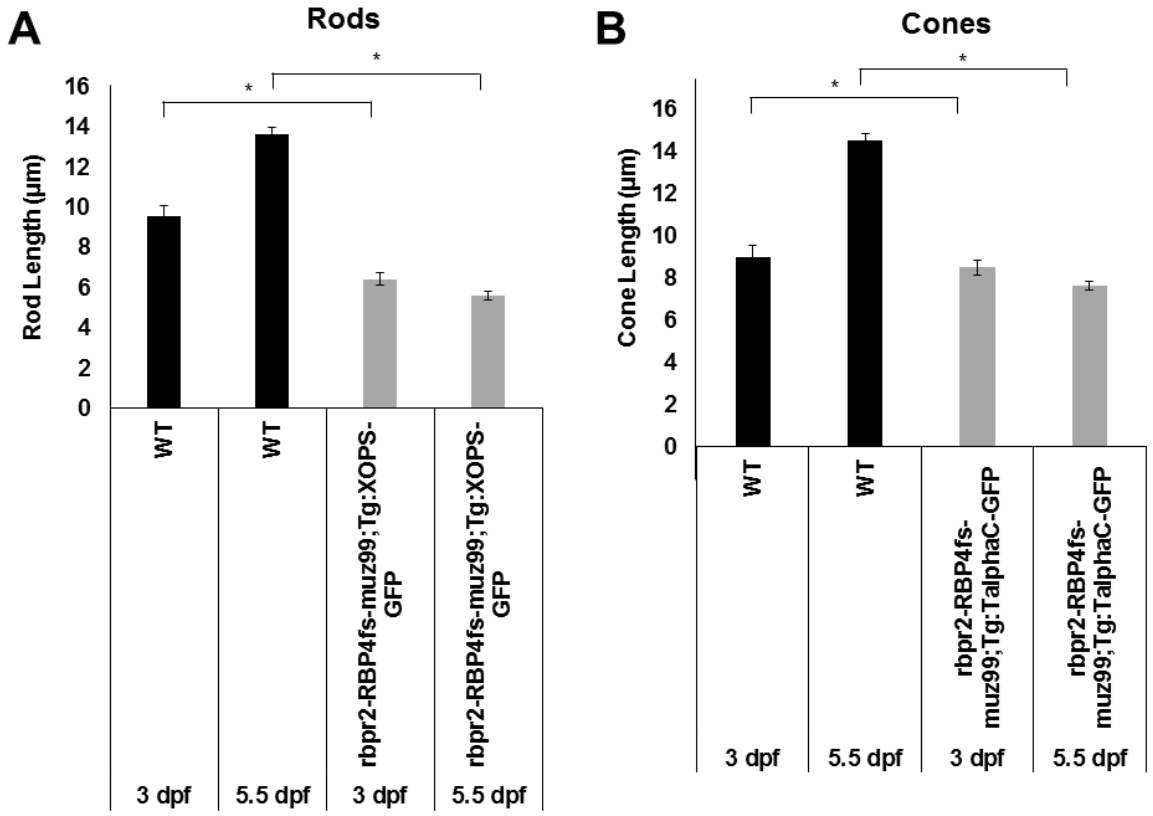

Figure S8. Quantification of photoreceptor length in *rbpr2*$^{fs\text{-}muz99}$ mutant animals. Image J was used to quantify and measure GFP staining along the length of the photoreceptors (from the photoreceptor synapse to the apical edge of the inner segment) in rods (**A**) and cones (**B**) in both WT and *rbrp2*-mutant animals at 3 dpf and 5.5 dpf time points. Approximately 150 cones and rods in WT and *rbpr2* mutant retinas were counted and sized.

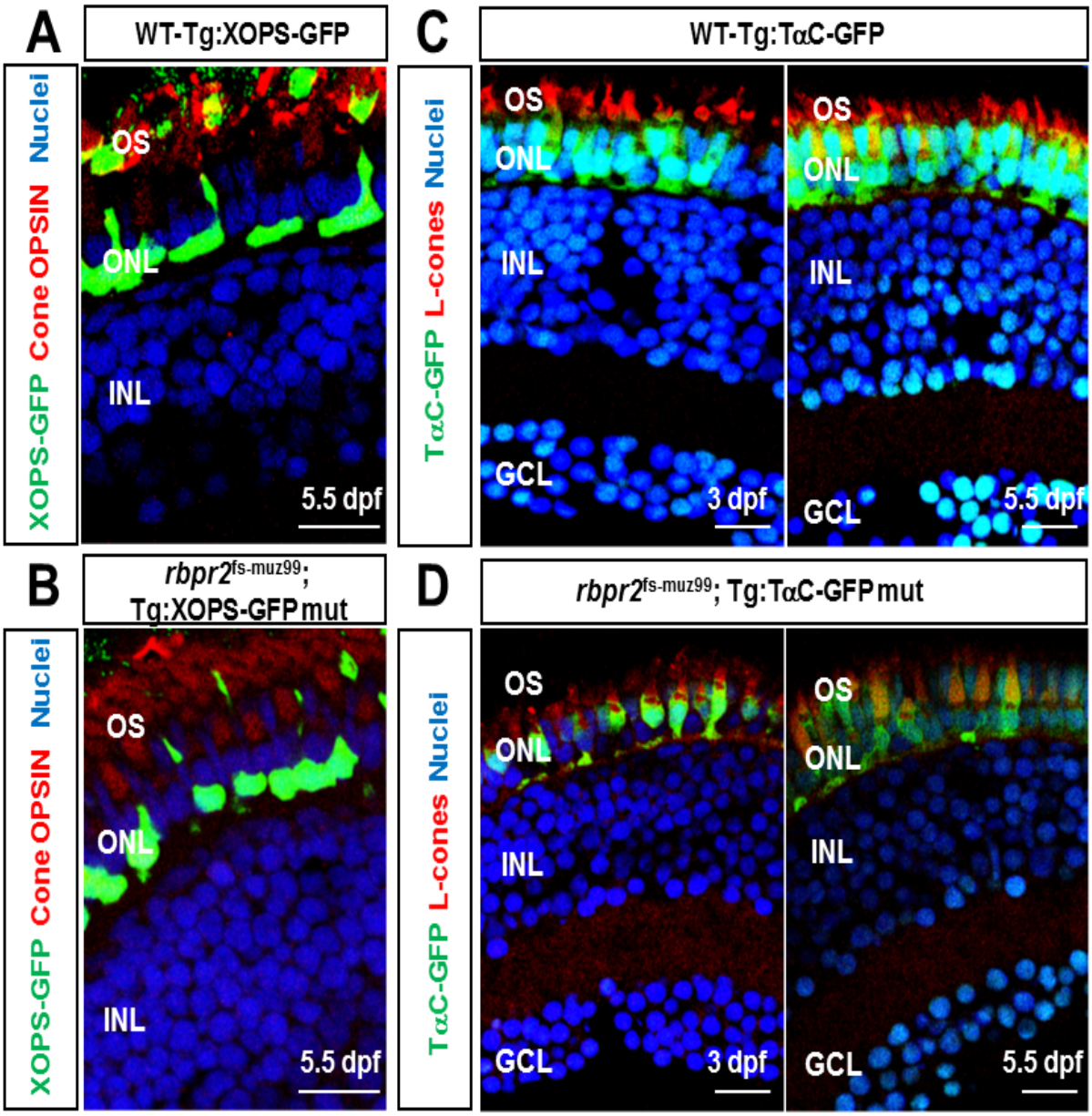

Figure S9. Counterstaining in transgenic *rbpr2*$^{fs\text{-}muz99}$ mutants. (**A, B**) WT-Tg:XOPS-GFP and *rbpr2*$^{fs\text{-}muz99}$;Tg:XOPS-GFP mutant retinas that express GFP in rods only were counter stained with R/G cone opsin antibody followed by Alexa 594. (**C, D**) WT Tg:TαC-GFP and *rbpr2*$^{fs\text{-}muz99}$;Tg:TαC-GFP mutant retinas that express GFP in cones only were counter stained with 1D4 (L-cones) antibody followed by Alexa 594. Nuclei were stained with DAPI. (**A, B**) scale bar=50µm; (**C, D**) scale bar=75µm. OS, outer segments; INL, Inner nuclear layer; ONL, Outer nuclear layer; dpf, days post fertilization; IS, Inner segments.

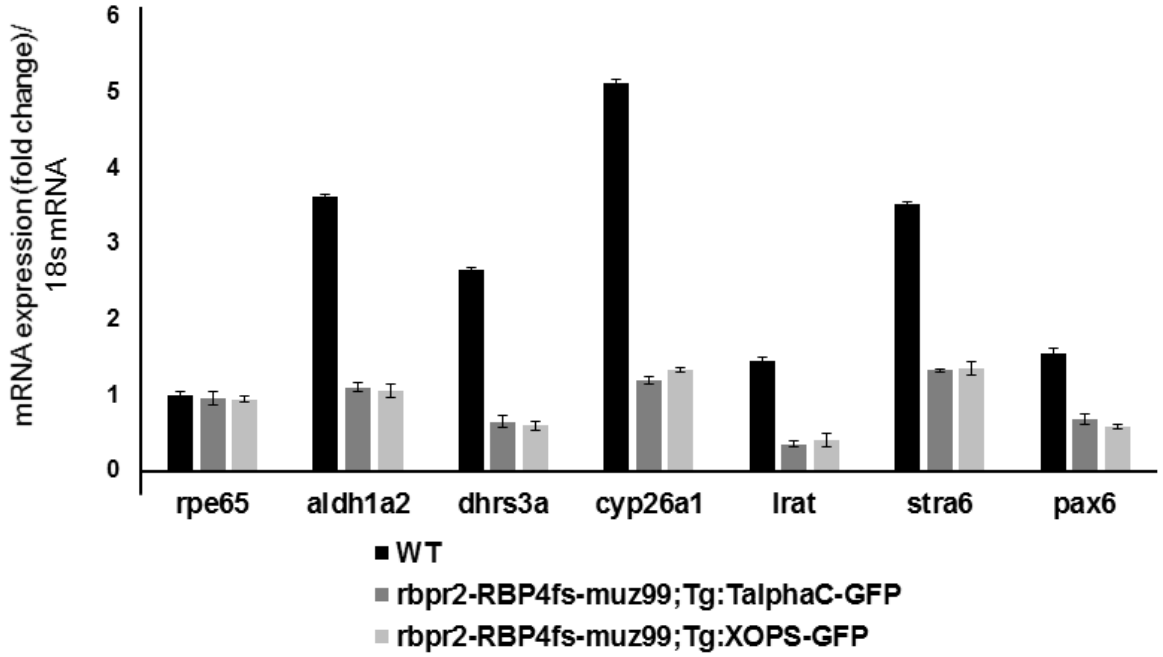

Figure S10. Downregulation of retinoid signaling regulated genes in *rbpr2*$^{fs\text{-}muz99}$ mutant zebrafish eyes.

Retina-specific gene expression dependent on RA signaling were compared by qPCR using equal amounts of total RNA from heads of wild-type/ control (black bars) and *rbpr2* $^{fs\text{-}muz99}$ mutants (grey bars) at 3.5 dpf. Rpe65 mRNA expression values were set to 1 and difference in gene expression between the two genotypes are shown as relative fold change normalized to endogenous 18S RNA. *p<0.005.

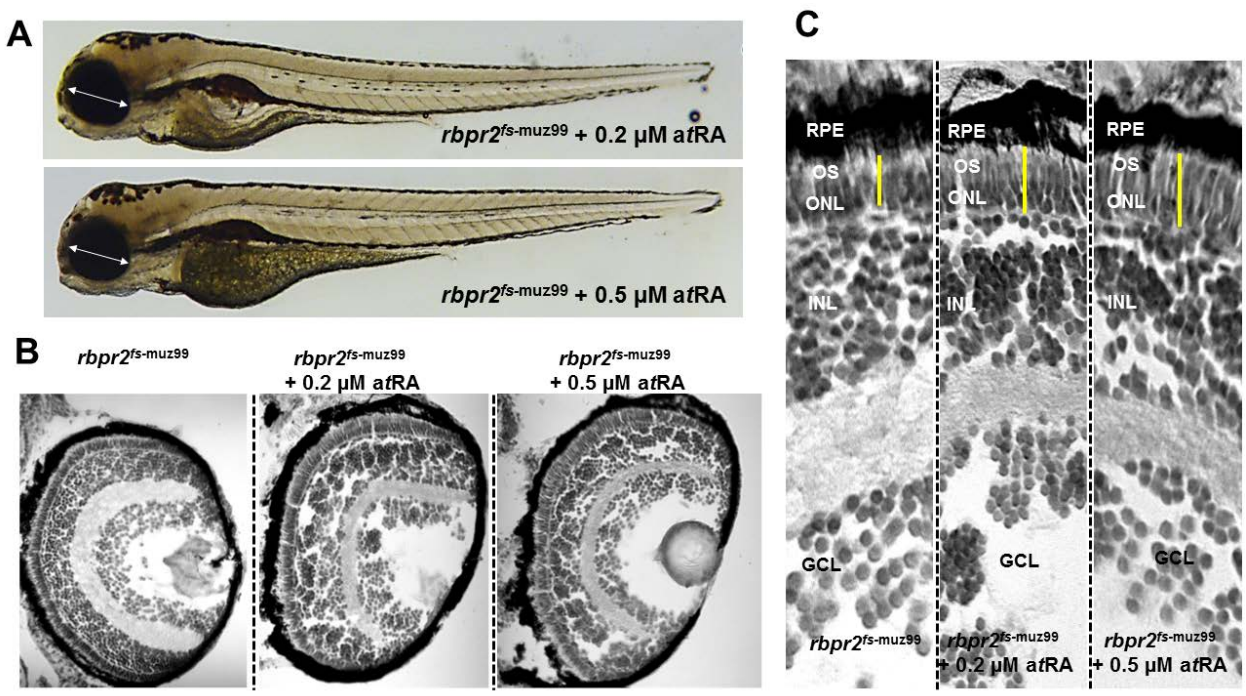

Figure S11. All-*trans* retinoic acid rescues the *rbpr2*$^{fs\text{-}muz99}$ mutant phenotype.

(**A**) Dose specific treatment with all-*trans* retinoic acid (a*t*RA) rescues the *rbpr2*$^{fs\text{-}muz99}$ mutant phenotype. Images obtained at 5-5.5 dpf. Rescue experiments of *rbpr2* mutants with either mRNA or a*t*RA were repeated twice as outlined in methods. (**B, C**) Representative images of eye sections from *at*RA treated *rbpr2*$^{fs\text{-}muz99}$ mutants at 5.5 dpf. RPE, retinal pigmented epithelium; OS, outer segments; INL, inner nuclear layer; ONL, outer nuclear layer; dpf, days post fertilization.

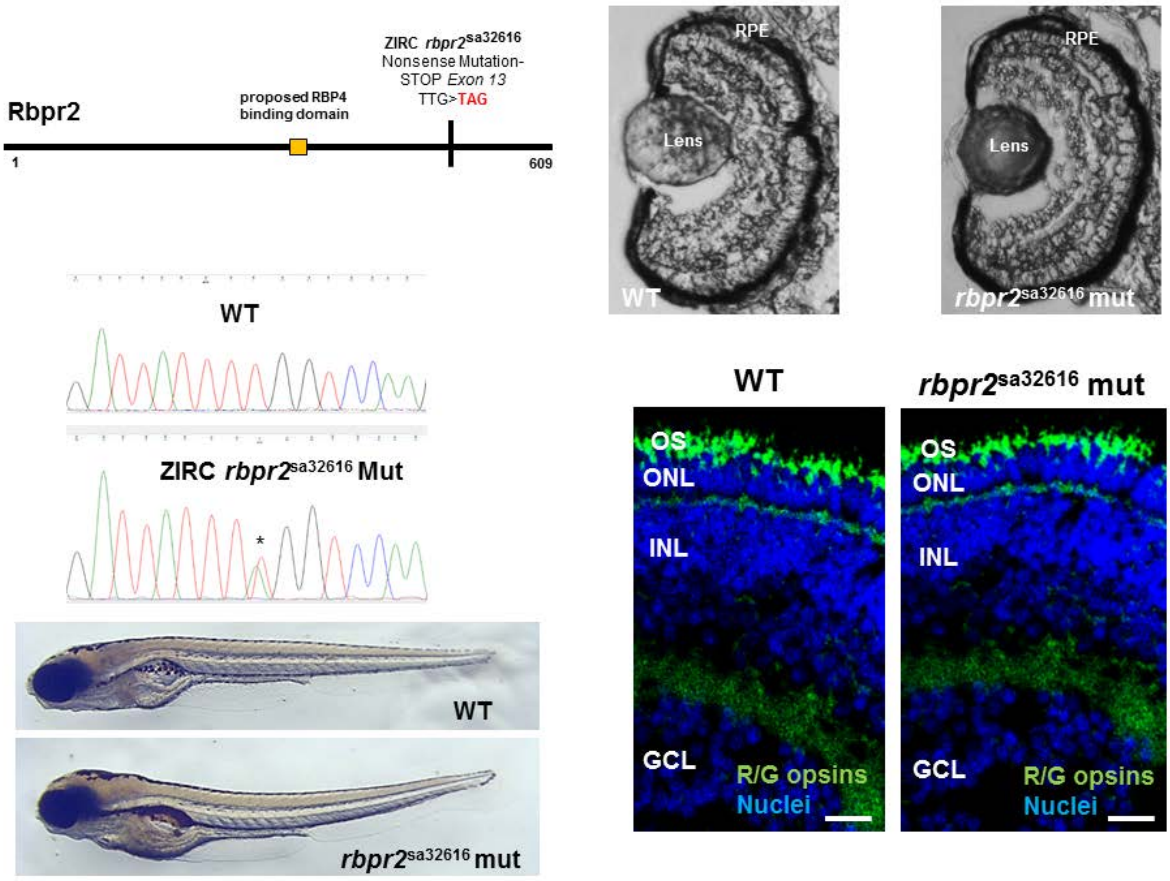

Figure S12. ZIRC *rbpr2* mutants (*rbpr2*^{sa32616}) encompassing a mutation after the proposed RBP4 binding sites in Rbpr2 do not show eye phenotypes.

A *rbpr2* mutant zebrafish line (G>A mutation; *rbpr2*^{sa32616}) from the Zebrafish International Resource Center (ZIRC) which results in a premature stop codon in exon 13, was obtained and analyzed by light microscopy, histology and immunohistochemistry at 5.5 dpf. With the exception of a curved/ bent tail, no other significant phenotype was observed in this zebrafish *rbpr2*-mutant. Note: The TTG>TAG mutation in exon 13 of the Rbpr2 coding sequence occurs “after” the proposed RBP4 binding sites. Immunostaining for cone photoreceptors (R/G opsins antibody) revealed that cones in both WT and mutants at 5.5 dpf were similar in number and showed normal morphology. OS, outer segments; IS, inner segments; PRL, photoreceptor cell layer; ONL, outer nuclear layer; INL, inner nuclear layer; GCL, ganglion cell layer; WT, wild-type; dpf, days post fertilization.